

Optimum Operation of Asymmetrical-Cells-Based Linear Doherty Power Amplifiers—Uneven Power Drive and Power Matching

Jangheon Kim, Jeonghyeon Cha, Ildu Kim, and Bumman Kim, *Senior Member, IEEE*

Abstract—We developed a Doherty amplifier with uneven input drive and optimized individual matching for the carrier and peaking cells. In the proposed amplifier, higher input power is delivered to the peaking cell rather than the carrier cell for optimized linear power operation, especially for appropriate load modulation. Both cells are matched differently to further optimize the performance. We analyzed the efficiency of the proposed amplifier as a function of the input drive ratio for the two cells. To interpret the linearity related to the load modulation and harmonic cancellation mechanisms, we simulated the third-order intermodulation amplitude and phase of each cell of the proposed amplifier. For verification, we implemented the asymmetric power amplifier with uneven drive and optimized power matching using Motorola's MRF281SR1 LDMOSFET with a 4-W peak envelope power. For a 2.14-GHz forward-link wireless code-division multiple-access signal, the measured drain efficiency of the amplifier is 40%, and the measured average output power is 33 dBm at an adjacent channel leakage ratio (ACLR) of -35 dBc, while those of the comparable class-AB amplifier are 21% and 30.6 dBm at the same ACLR level, respectively.

Index Terms—Adjacent channel leakage ratio (ACLR), asymmetric power amplifier, Doherty amplifier, efficiency, linearity, linear power amplifier (LPA).

I. INTRODUCTION

IN CURRENT wireless communication systems, the physical size of the linear power amplifier (LPA) of a base station is becoming more and more compact. It is thus necessary to develop amplifiers with high efficiency and good linearity to counteract the thermal problem created by the smaller size. A Doherty amplifier is the most promising candidate for the application [1]–[16].

The simplest Doherty amplifier operation can be achieved using two cells with a class-AB biased carrier amplifier cell and a class-C biased peaking amplifier cell. Due to its lower bias point, the current level of the peaking cell is always lower than that of the carrier cell. The load impedances of both cells cannot be fully modulated to the value of the optimum impedance for a high power match. Thus, neither cell can generate its respective full power. Bias adaptation for the Doherty amplifier is a

good approach to solve this problem. As the magnitude of the instantaneous input signal increases, the gate bias voltage of the peaking cell increases according to the envelope of the signal. Therefore, it is possible to achieve a perfect Doherty operation. However, it needs an external voltage control circuitry, which adds to its complexity [2], [3].

The objective of this paper is to overcome such a problem without any external circuitry. We propose an uneven power drive for the carrier and peaking cells. In the proposed amplifier, the input power is split into two uneven powers, the peaking cell taking more power than the carrier cell. Similar to the bias adaptation approach, the fundamental currents of both cells can be the same at the full power level. As a result, the impedances of both cells are fully modulated to the value of the optimum power matching at the high power level and maximum power is delivered to the common load. We have also found the optimal matching impedances of each cell for a highly linear power operation. We will explain the circuit configuration, operation characteristics, and optimum efficiency and linearity operation conditions of the proposed amplifier. For verification, the amplifier is simulated, implemented, and tested at a 2.14-GHz center frequency. The implemented amplifier is quite simple and its measurement results show excellent performance.

II. ANALYSIS FOR OPERATION CHARACTERISTICS

A. Current Generation Ratio of Peaking Versus Carrier Cells

The LPA based on the asymmetrical power cells, commonly called a Doherty amplifier, consists of a class-AB biased carrier amplifier cell and a class-C biased peaking amplifier cell. Usually, both cells have identical size, matching circuits, and input drives. In addition, since the bias point of the peaking cell is lower than that of the carrier cell, the current of the peaking cell at maximum input drive reaches below the maximum allowable current level. Fig. 1 illustrates the current level of a general amplifier at the maximum drive as a function of conduction angle. This figure is given in [1, p. 49, Fig 3.2].

In Fig. 1, the current level is normalized to the maximum channel current and the operation regions for classes AB and C are also indicated. As shown, the fundamental component of the current is limited by

$$I_1 = \begin{cases} 0.5 \sim 0.536, & \alpha = \pi \sim 2\pi \\ 0 \sim 0.5, & \alpha = 0 \sim \pi. \end{cases} \quad (1)$$

Manuscript received September 29, 2004; revised November 19, 2004. This work was supported by the Korean Ministry of Education under Brain Korea 21 projects.

The authors are with the Department of Electronic and Electrical Engineering, Pohang University of Science and Technology, Pohang, Gyungbuk 790-784, Korea (e-mail: rage3k@postech.ac.kr).

Digital Object Identifier 10.1109/TMTT.2005.847073

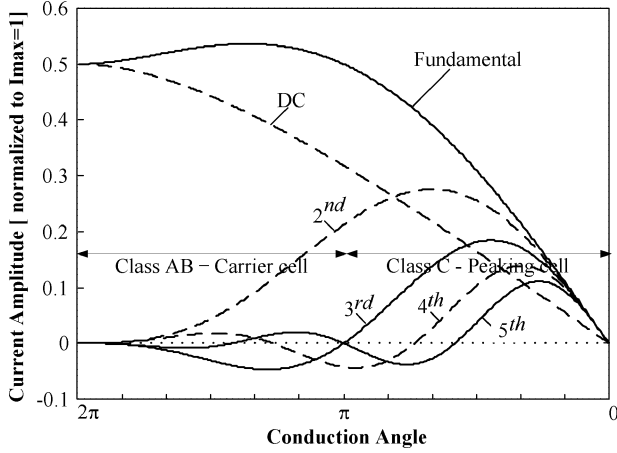


Fig. 1. Harmonic components of the conduction current versus conduction angle.

The fundamental components of the channel currents at the maximum drive for the cells $I_{1,C}$ and $I_{1,P}$ are given by the following expression [1]:

$$I_{1,C} = \frac{I_{\max}}{2\pi} \cdot \frac{\alpha_c - \sin \alpha_c}{1 - \cos\left(\frac{\alpha_c}{2}\right)}$$

$$I_{1,P} = \frac{I_{\max}}{2\pi} \cdot \frac{\alpha_p - \sin \alpha_p}{1 - \cos\left(\frac{\alpha_p}{2}\right)} \quad (2)$$

where α_c is the conduction angle of the carrier cell and α_p is the conduction angle of the peaking cell.

Due to the class-C bias of the peaking cell, it is not fully driven even at the maximum input for the carrier cell, and we define the current ratio of the two cells at the maximum drive for the amplifier as

$$\sigma = \frac{I_{1,C}}{I_{1,P} \cdot (1 - N)} \quad (3)$$

where N denotes the portion of the voltage where the peaking cell starts to conduct. Therefore, $I_{1,P} \cdot (1 - N)$ describes the fundamental current level of the peaking cell at the maximum input drive for the carrier cell.

The output power ratio from the two cells in decibel E_I is given by

$$E_I = 10 \log(\sigma^2) = 10 \log\left(\frac{I_{1,C}}{I_{1,P}}\right)^2 + 10 \log\left\{\frac{1}{(1 - N)^2}\right\}. \quad (4)$$

Note that E_I is the criterion to determine the under-drive ratio of the peaking power, which is related to the load modulation. If $I_{1,C} = 0.52$ ($\alpha_c = 200^\circ$) and $I_{1,P} = 0.44$ ($\alpha_p = 140^\circ$), for example, the load could be modulated fully by increasing the drive power for the peaking cell (in this case, N is 0.5) by 7.6 dB ($\sigma = 2.4$), as determined from the (4).

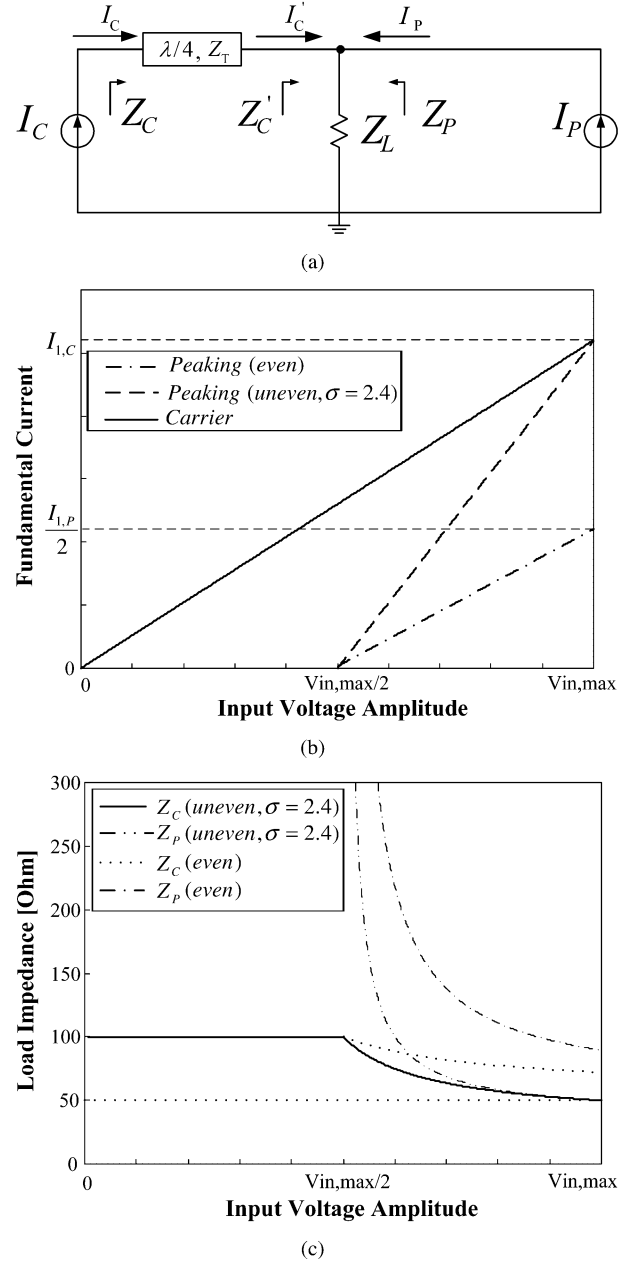


Fig. 2. (a) Operational diagram of the asymmetric cell amplifier with uneven power drive. (b) Fundamental currents versus input voltage. (c) Load impedances versus input drive for even and uneven ($\sigma = 2.4$) drives (carrier ($\alpha_c = 200^\circ$), peaking ($\alpha_p = 140^\circ$), $N = 0.5$, $Z_0 = 50 \Omega$, and $Z_T = 50 \Omega$).

B. Efficiency of the Asymmetric Cell Amplifier With Uneven Power Drive

The fundamental operation principle and efficiency analysis of the Doherty amplifier have been well described in previous literature [1], [4], [9]. To enhance the output power from the peaking cell, we propose an amplifier with uneven power drive, applying more power to the peaking cell. Fig. 2(a) shows an operational diagram to analyze efficiency of the amplifier with an uneven drive σ times larger current source for the peaking cell. It is assumed that each current source is linearly proportional to the input voltage signal and they contain ideal harmonic short circuits so that the efficiency analysis can be carried out using

the fundamental and dc components only. Fig. 2(b) shows the fundamental currents from the two cells for even and uneven drives ($\sigma = 2.4$). As shown, the carrier is biased at class AB and the peaking at C, half of the maximum voltage ($V_{in,max}$) below class B. As shown in Fig. 2(c), in the case of an uneven power drive ($\sigma = 2.4$), we can achieve the appropriate load modulation suggested by Doherty since the cells of the proposed amplifier generate equal power.

From Fig. 2(b), the currents from the carrier and peaking cells are given by

$$I_C = \frac{I_{1,C}}{V_{in,max}} \cdot v_{in}, \quad 0 < v_{in} < V_{in,max} \quad (5)$$

$$I_{P,even} = \begin{cases} I_{1,P} = 0, & 0 < v_{in} < N \cdot V_{in,max} \\ \left(\frac{I_{1,P}}{V_{in,max}} \right) \cdot v_{in} - N \cdot I_{1,P}, & N \cdot V_{in,max} < v_{in} < V_{in,max} \end{cases} \quad (6)$$

$$I_{P,uneven} = \begin{cases} \sigma I_{1,P} = 0, & 0 < v_{in} < N \cdot V_{in,max} \\ \left(\frac{\sigma I_{1,P}}{V_{in,max}} \right) \cdot v_{in} - N \cdot \sigma I_{1,P}, & N \cdot V_{in,max} < v_{in} < V_{in,max} \end{cases} \quad (7)$$

where $I_{P,even}$ is the current level of the peaking cell with an even power drive, and $I_{P,uneven}$ is the current level of the peaking cell with an uneven power drive.

Next, the load impedances of the two cells are given by

$$Z_C = \begin{cases} \frac{Z_T^2}{Z_L}, & 0 < v_{in} < N \cdot V_{in,max} \\ \frac{Z_T^2}{\left[Z_L \cdot \left(1 + \frac{I_P}{I_C} \right) \right]}, & N \cdot V_{in,max} < v_{in} < V_{in,max} \end{cases} \quad (8)$$

$$Z_P = \begin{cases} \infty, & 0 < v_{in} < N \cdot V_{in,max} \\ Z_L \left(1 + \frac{I_C}{I_P} \right), & N \cdot V_{in,max} < v_{in} < V_{in,max} \end{cases} \quad (9)$$

At the low-power region ($0 < v_{in} < N \cdot V_{in,max}$), where only the carrier cell is active, the RF and dc powers increase according to the input drive voltage. If we use $Z_T = Z_0$ and $Z_L = Z_0/2$, the RF power and dc power are given by

$$\begin{aligned} P_{RF} &= \frac{1}{2} I_C^2 Z_C \\ &= \frac{1}{2} \left(\frac{v_{in} \cdot I_{1,C}}{V_{in,max}} \right)^2 \cdot 2Z_0 \\ &= I_{1,C} \left(\frac{v_{in}}{V_{in,max}} \right)^2 \cdot V_{dc} \end{aligned} \quad (10)$$

$$\begin{aligned} P_{dc} &= I_{dc,C} \cdot V_{dc} \\ &= I_{dc,C} \left(\frac{v_{in}}{V_{in,max}} \right) \cdot V_{dc} \end{aligned} \quad (11)$$

where V_{dc} is the bias voltage of each cell.

From (10) and (11), the efficiency becomes

$$\eta = \frac{P_{RF}}{P_{dc}} \times 100 = \frac{I_{1,C}}{I_{dc,C}} \left(\frac{v_{in}}{V_{in,max}} \right) \times 100. \quad (12)$$

At the higher power region ($N \cdot V_{in,max} < v_{in} < V_{in,max}$), both cells are active. Thus, the RF and dc powers are the sum of the two cells and are given by (13) and (14). Thus, the efficiency is given by

$$\begin{aligned} P_{RF} &= \frac{1}{2} (I_C^2 Z_C + I_P^2 Z_P) \\ &= V_{dc} \cdot \left[\frac{I_{1,C}^2 \cdot V^3}{(I_{1,C} + \sigma I_{1,P}) \cdot V - N \cdot \sigma I_{1,P}} \right. \\ &\quad \left. + \frac{\sigma I_{1,P} (V - N) \{ (I_{1,C} + \sigma I_{1,P}) V - N \cdot \sigma I_{1,P} \}}{4 I_{1,C}} \right] \end{aligned} \quad (13)$$

$$\begin{aligned} P_{dc} &= (I_{dc,C} + I_{dc,P}) \cdot V_{dc} \\ &= [I_{dc,C} \cdot V + \sigma I_{dc,P} (V - N)] \cdot V_{dc} \end{aligned} \quad (14)$$

where $I_{dc,C}$ is the dc current of the carrier cell and $I_{dc,P}$ is the dc current of the peaking cell at the maximum drive

$$\begin{aligned} \eta &= \frac{P_{RF}}{P_{dc}} \times 100 \\ &= \left[\frac{I_{1,C}^2 \cdot V^3}{(I_{1,C} + \sigma I_{1,P}) \cdot V - N \cdot \sigma I_{1,P}} \right. \\ &\quad \left. + \frac{\sigma I_{1,P} (V - N) \{ (I_{1,C} + \sigma I_{1,P}) V - N \cdot \sigma I_{1,P} \}}{4 I_{1,C}} \right] \\ &\quad \div [I_{dc,C} V + \sigma I_{dc,P} (V - N)] \times 100 \end{aligned} \quad (15)$$

where

$$\begin{aligned} Z_0 &= \frac{V_{dc}}{I_{1,C}} \\ V &= \frac{v_{in}}{V_{in,max}} \\ I_{dc,C} &= \frac{I_{max}}{2\pi} \cdot \frac{2 \sin \left(\frac{\alpha_c}{2} \right) - \alpha_c \cos \left(\frac{\alpha_c}{2} \right)}{1 - \cos \left(\frac{\alpha_c}{2} \right)} \\ I_{dc,P} &= \frac{I_{max}}{2\pi} \cdot \frac{2 \sin \left(\frac{\alpha_p}{2} \right) - \alpha_p \cos \left(\frac{\alpha_p}{2} \right)}{1 - \cos \left(\frac{\alpha_p}{2} \right)}. \end{aligned}$$

Fig. 3(a) shows the calculated efficiencies based on the above analysis for $\alpha_c = 180^\circ \sim 360^\circ$ and $\alpha_p = 140^\circ$ with an uneven power drive ($\sigma = 2.3 \sim 2.46$). At the low-power region, the load impedance of the carrier cell is two times larger than that of a conventional class-AB amplifier. The carrier cell reaches the saturation state at input voltage of $V_{in,max}/2$ since the maximum fundamental current swing is half and the maximum voltage swing reaches to V_{dc} , as shown in Fig. 3(b) and (c). As a result, the maximum power level is half of the carrier cell's allowable power level, and the efficiency of the amplifier is equal to the

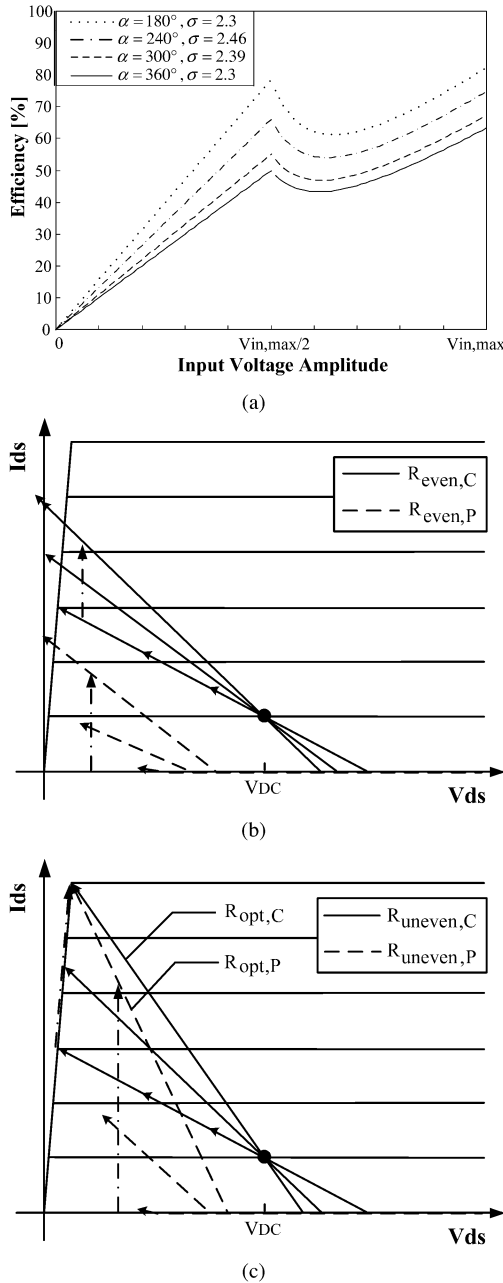


Fig. 3. (a) Efficiency versus input drive level for the amplifier with uneven power drive. [$\alpha_c = 180^\circ \sim 360^\circ$ and $\alpha_p = 140^\circ$ with uneven power drive ($\sigma = 2.3 \sim 2.46$)] load lines of each cell for: (b) even power drive and (c) uneven power drive.

maximum efficiency of the carrier cell given by (12). Fig. 3(b) represents the load lines of the two cells with an even power drive at a high-power level. It is shown that the voltage swing of the carrier cell is larger than the allowable maximum voltage swing of V_{dc} due to the high load impedance. The peaking cell produces a current far less than the full capability with voltage swing larger than V_{dc} . Thus, it is clear that the two cells of a conventional Doherty amplifier are heavily saturated, degrading the linearity at the full power drive and producing far less power. However, for equal output current operation by an uneven drive, the load line of the carrier cell follows the knee current without producing saturation due to proper load modulation, as shown in Fig. 3(c). The voltage swing of the peaking cell increases in

proportion to the power level and reaches the maximum voltage swing of V_{dc} only at maximum power. At the maximum power level, both cells have optimum matching impedances, as shown in Fig. 3(c). Therefore, the asymmetric power amplifier with uneven drive operates more linearly and produces more power than an even drive.

C. Linearity of the Asymmetric Cell Amplifier With Uneven Power Drive

The linearity of the amplifier is more complicated than that of a class-AB amplifier. In the low-power region, the linearity of the amplifier is entirely determined by the carrier cell. Therefore, the carrier cell should be highly linear for the high load impedance.

In the high-power region, the current level of the peaking cell plays an important role in determining the load modulation of the amplifier. Fig. 2(c) shows the impedance level through the load modulation [see (8) and (9)]. For the asymmetric amplifier with even power drive, the fundamental current of the peaking cell is insufficient to achieve the full load modulation. The load impedances of both cells are larger than the optimum values in the high-power region, as shown in Fig. 3(b). As a result, the carrier and peaking cells are driven into saturation without either producing full power. Thus, the amplifier is seriously affected by linearity, as well as power level.

For the amplifier with uneven power drive, the linearity of the amplifier is improved due to proper power operation without severe saturation. The linearity is further enhanced by the harmonic cancellation of $gm3$ from the two cells at appropriate gate biases [6], [7]. The carrier cell, which is biased at class AB, has the gain compression at high output power levels, while the class-C biased peaking cell has the gain expansion. Hence, the gain expansion of the peaking cell can compensate the gain compression of the carrier cell. Specifically, the third-order intermodulation (IM3) level from the carrier cell increases and the phase of IM3 is decreased because the gain of the carrier cell is compressed. By contrast, when the gain of the peaking cell is expanded, both the IM3 level and phase increase. To cancel out IM3s from the two cells, the components must be 180° out-of-phase with the same amplitudes. Therefore, the peaking cell should be designed appropriately to cancel the harmonics of the carrier cell.

D. Optimum Matching Impedances for the Two Cells

As shown in Fig. 2, the fundamental current level of the peaking cell is insufficient to fully modulate the load impedance, and both cells see larger load impedances than the design ones. To achieve a highly linear amplifier, the load impedances of the carrier and peaking cells must be reduced appropriately for better linearity and also for proper power matching. Especially because the bias point of the peaking cell is lower than that of the carrier cell, the load impedances of the peaking cell must be reduced more than that of the carrier cell, as shown in Fig. 3(c).

For the amplifier design, each cell must be highly linear minimizing the IM3 levels because IM3 cancellation is limited. For the cancellation, the IM3s of both cells must be 180° out-of-phase with the same amplitudes over the appropriate

power level. Thus, in the high power region, the load impedances of the cells must be reduced for highly linear operation. However, biases of the cells have to be properly adjusted (lower value than normal) for optimal cancellation and improved efficiency.

III. SIMULATION RESULTS

In Section II, we analyzed the efficiency and linearity of the proposed amplifier. The analysis was simplified by using ideal current sources and it does not include detailed behaviors of real devices. To search for the exact behaviors of the amplifier, we performed on ADS simulation using Ericsson's model PTF10107 LDMOSFET. The uneven input drive was adjusted by an ideal two-way power splitter with uneven power ratio of 1 : 1.6 and 1 : 2.5. A quiescent current of the carrier cell was set to 70 mA, and the gate voltage of the peaking cell was fixed at 1 V. The drain bias voltage was $V_{DD} = 26$ V.

A. Continuous Wave (CW) Test of the Proposed Amplifier

Fig. 4(a) shows the fundamental currents of the two cells as a function of the output power level for the even input drive (1 : 1), the uneven input drive (1 : 1.6, 1 : 2.5) and the optimum matching for the even drive. As the uneven power drive ratio increases, the current of the peaking cell increases and that of the carrier cell decreases, resulting in an operation more like an ideal Doherty amplifier. For the optimum uneven power drive, the currents from the two cells become equal at approximately $P1$ dB. As the load impedances of both cells are reduced for optimum power matching, the currents of both cells also increase slightly.

We also explored the load impedances of the two cells as a function of output power [shown in Fig. 4(b)]. In the low-power region, the impedance of the carrier cell is approximately 100Ω , and the load impedance of the peaking cell is very high at the conduction starting point. The load impedances of each cell are reduced as the power level increases. At the uneven power drive ratio of 2.5, the load impedances of the two cells approach close to 50Ω at approximately $P1$ dB. The optimum load impedances of the cells for the even drive also move closer to approximately 50Ω . As the uneven power drive ratio increases, the carrier cell is compressed early and the peaking cell expanded early and the region is wider than the usual Doherty amplifier, as shown in Fig. 4(c). Therefore, the asymmetric amplifier with an uneven drive generates more linear power because the early gain expansion of the peaking cell compensates the gain compression of the carrier cell over the wide power range.

B. Two-Tone Test of the Proposed Amplifier

Fig. 5(a) show the amplitude characteristics of IM3 verse the output power, and Fig. 5(b) represents the phase difference (phase of the peaking cell—phase of the carrier cell) of IM3 verse output power. First, we explored the typical class-AB amplifier. The phase and amplitude variations are rather slow and IM3s from the two cells add up, as shown in Fig. 5(c). Second, for an asymmetric amplifier with even drive, IM3 amplitudes and phases of the carrier and peaking cells are quite different at a low power. As the output power increases, the phase of the carrier cell increases, while that of the peaking cell decreases.

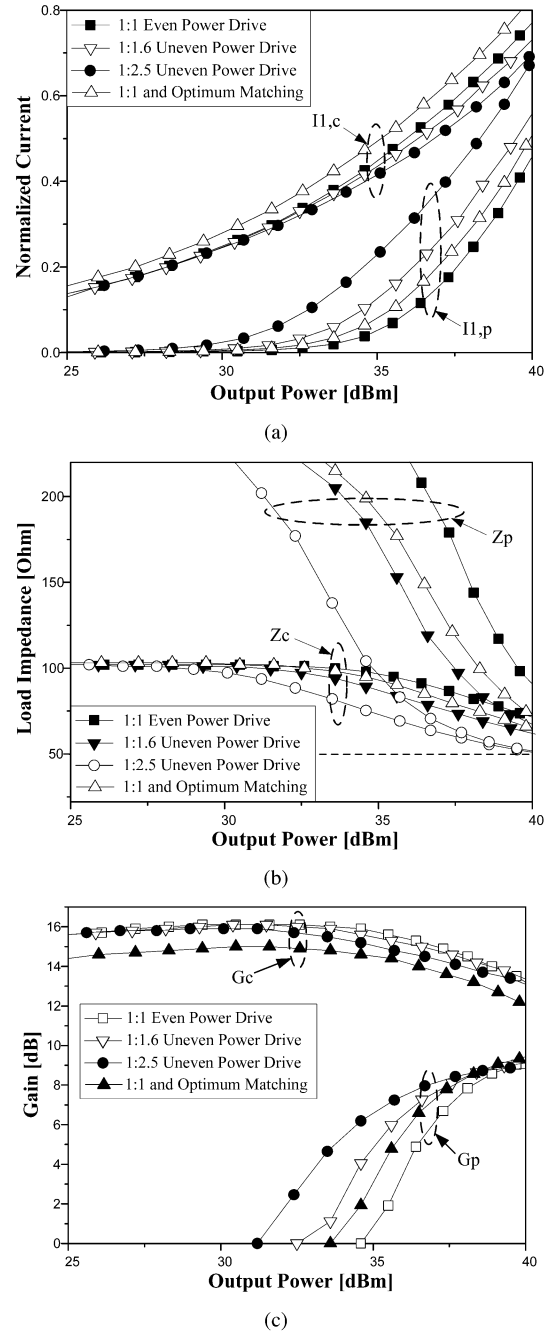


Fig. 4. Simulated results for the amplifier with even and uneven power drives and optimum power matching. (a) Normalized currents. (b) Load impedances. (c) Power gains.

Above some high output power level, the phases from the two cells are maintained and the difference is approximately 180° . Thus, IM3s from the two cells are cancelled. However, the phase difference of 180° can be achieved through only a small dynamic range and IM3 levels in the range are a little different. Third, we investigated an amplifier with uneven drive. As the uneven power drive ratio increases, IM3s have a phase difference of 180° even at low output power levels. Besides, IM3 levels are quite similar at the low-power level. Thus, the proposed amplifier can cancel IM3 better and have better linear characteristics.

Finally, we inspected the characteristics of an amplifier with even drive for power-matching variation. We could find the load

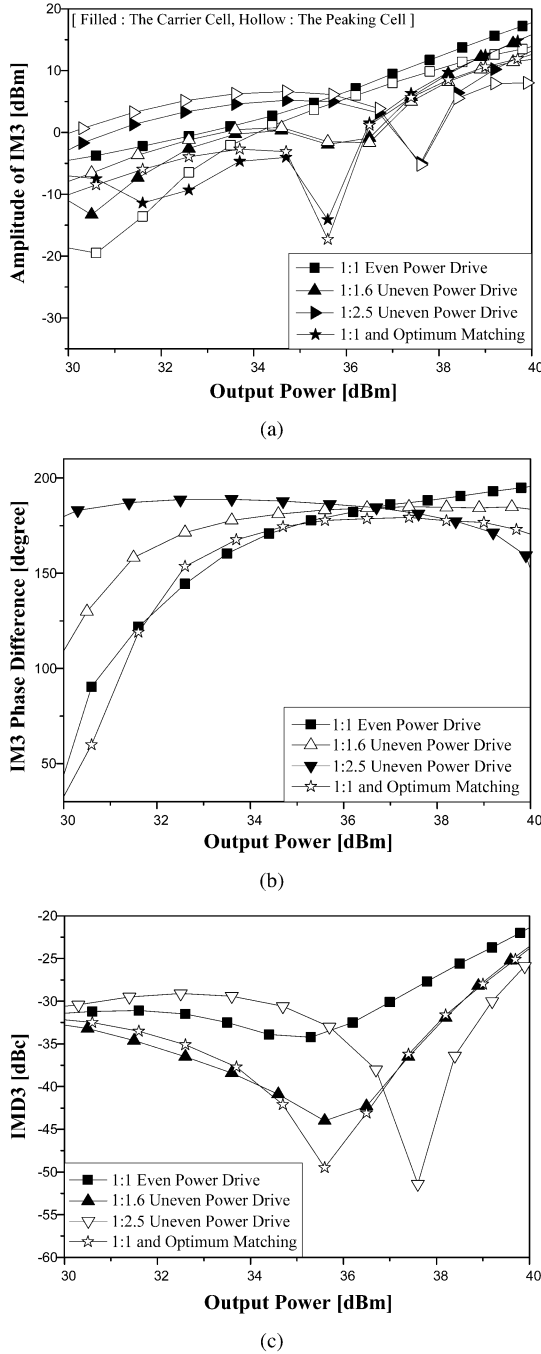


Fig. 5. Two-tone simulated results of the amplifier with various conditions. (a) Amplitude of IM3. (b) Phase difference of IM3. (c) Third-order intermodulation distortion (IMD3).

that produced more favorable phase and amplitude characteristics. As expected, the impedance is lower than the normal Doherty amplifier matching impedance. We emphasized that, for a linear amplifier, the carrier cell should be highly linear, as well as have an appropriate load modulation. Since this IM3 cancellation is limited, it is also important to reduce IM3 levels of the two cells.

IV. IMPLEMENTATIONS AND EXPERIMENTAL RESULTS

In Section III, we proposed an asymmetric cell amplifier with an uneven power drive. Fig. 6 shows a schematic diagram

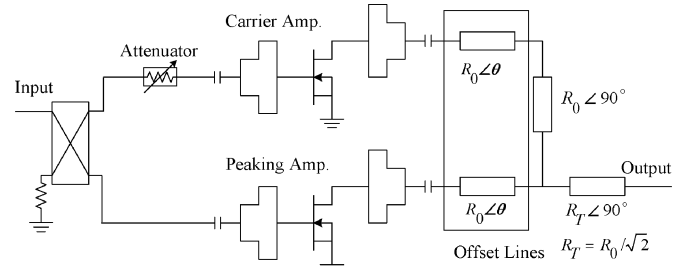


Fig. 6. Schematic diagram of the proposed amplifier.

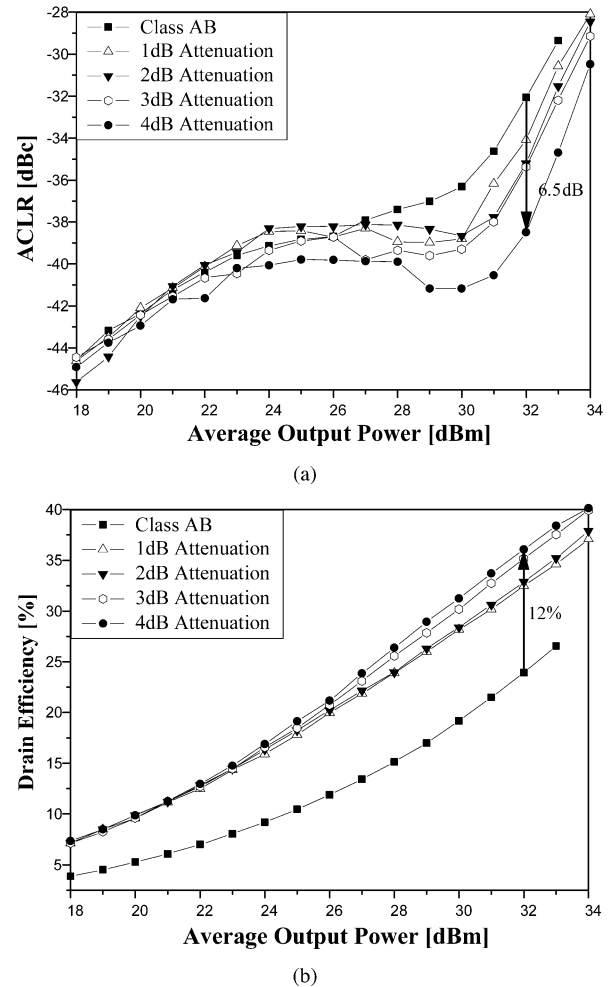


Fig. 7. Measured performance of the amplifier with uneven power drive and class-AB amplifier for a 2.14-GHz forward-link WCDMA signal. (a) ACLR. (b) Drain efficiency.

of the proposed amplifier, which is composed of an uneven power divider adjusted by an attenuator, fully matched carrier and peaking cells, offset lines, and a quarter-wave transformer. A hybrid coupler and π -attenuator are employed to create the uneven drive. We have fabricated the amplifiers with the power-matching variation to inspect the linearity and efficiency.

The carrier and peaking cells were designed using Motorola's MRF281SR1 LDMOSFET with a 4-W peak envelope power (PEP). The matching impedances for source and load are, respectively, $Z_S = 3.10 - j3.50 \Omega$ and $Z_L = 11.36 + j7.94 \Omega$. In the experiments, the suitable offset line for the peaking cell is 12.6° and the transformed output impedance is 344Ω [6], [11]. A quiescent bias for class AB is set to $I_{DS} = 20$ mA and

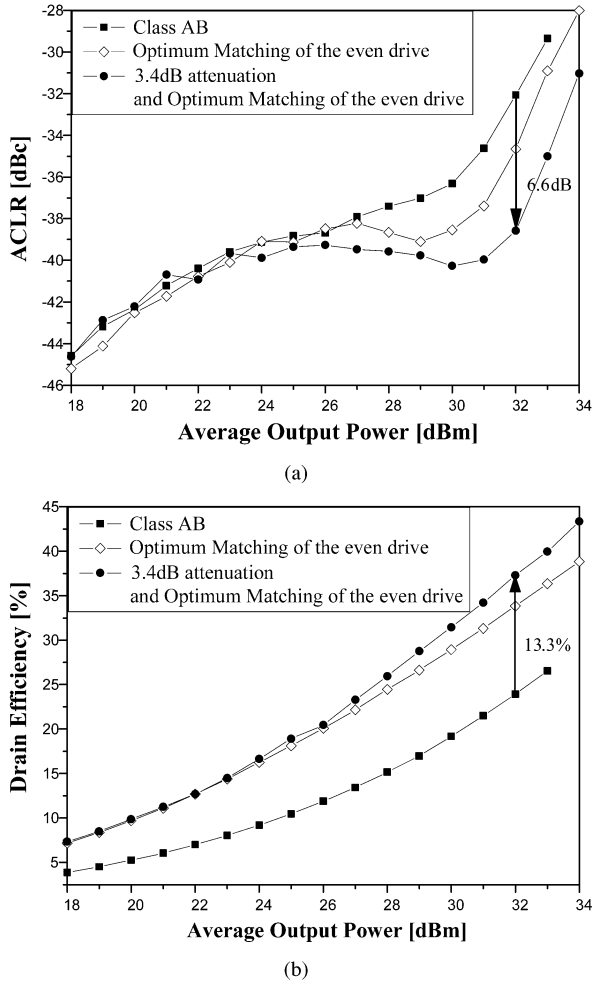


Fig. 8. Measured performance of the amplifier applying both techniques and class-AB amplifier for a 2.14-GHz forward-link WCDMA signal. (a) ACLR. (b) Drain efficiency.

$V_{DD} = 26$ V, and the amplifier is tuned for the best performance at the bias. The efficiency and linearity are optimized by adjusting the bias point of the peaking cell for each attenuation ratio.

Fig. 7(a) shows the measured adjacent channel leakage ratio (ACLR) of the amplifier with uneven drives and class-AB amplifier at offset 2.5 MHz for a 2.14-GHz forward-link wireless code-division multiple-access (WCDMA) signal. For the 4-dB attenuation at the carrier cell, the ACLR is improved by 6.5 dB compared to the class-AB amplifier at the output power of 32 dBm. Fig. 7(b) shows the measured drain efficiencies for the same condition and the drain efficiency is improved by 12.0%. As the attenuation ratio increases, the optimum gate bias voltage of the peaking cell is decreased. This result clearly shows that the proposed amplifier with uneven drive can provide good linearity, as well as high efficiency. The asymmetric cell amplifier with uneven power drive also generates full power from both cells.

The matching impedances of the cells are further optimized and the measured results for the ACLR and drain efficiency are depicted in Fig. 8. The optimized matching impedances are changed from $Z_L = 11.36 + j7.94 \Omega$ to $Z_{L,C} = 8.14 + j2.49 \Omega$, $Z_{L,P} = 7.55 + j4.88 \Omega$, where $Z_{L,C}$ and $Z_{L,P}$ are, respectively,

TABLE I
MEASURED PERFORMANCES AT ACLR = -35 dBc FOR
FORWARD-LINK WCDMA SIGNAL

	Output Power [dBm]	Efficiency [%]	$V_{G,P}$ [V]
Class AB	30.6	21	3.89 V / 3.92 V (20mA)
Uneven drive with 4dB attenuation	33	38.38	0 V
Optimum Matching	31.9	33	1.65 V
3.4dB att. and Optimum Matching	33	40	0 V

the output load impedances of the carrier and peaking cells. Fig. 8(a) shows the measured ACLRs of the amplifiers with the optimum power matching for the even and uneven drives, and class-AB amplifier at offset 2.5 MHz for a 2.14-GHz forward-link WCDMA signal. In comparison with the class-AB amplifier, the proposed amplifier with the uneven drive and optimum matching delivers significantly improved performances, the ACLR is reduced by 6.6 dB, and the drain efficiency is enhanced by 13.3% at an output power of 32 dBm. Additionally, the linearity specification of the base station is typically -55 dBc and, usually, the linearity is improved approximately 20 dB by linearizer such as feed-forward or digital predistorter. Thus, at an ACLR of -35 dBc, we have optimized the proposed amplifier for maximizing the efficiency and output power, and the results are summarized in Table I. The maximum average output power and efficiency of the amplifier applying both techniques is enhanced to 33 dBm and 40%, which represent 2.4 dB and 19% improvements over the class-AB amplifier. These results show that the proposed amplifier is suitable for the main amplifier of an LPA. Consequently, it is clear that our new amplifier is far superior to previous similar amplifiers.

V. CONCLUSIONS

For the optimized operation of the asymmetric amplifier, we have analyzed the fundamental current as a function of conduction angle and load modulation behavior. We have also derived the efficiency in terms of the reduced conduction angle. We have indicated the inappropriate load modulation for the conventional Doherty amplifier and have proposed an asymmetric power amplifier applying uneven power drive with matching impedance lower than usual amplifier. Besides, to investigate the mechanism for linearity improvement, we have clearly visualized IM3 cancellation behavior using a simulation of the amplifier.

To validate performances of the proposed amplifier experimentally, we have implemented the amplifier at 2.14 GHz using Motorola's MRF281SR1 LDMOSFET and have optimized it for the maximum average output power and drain efficiency at an ACLR of -35 dBc using a forward-link WCDMA signal. The maximum power and efficiency of the amplifier applying both techniques was enhanced to 33 dBm and 40%, which represent 2.4 dB and 19% improvements over the class-AB amplifier. For the proper operation of the amplifier, the carrier cell

should be highly linear for power operation, each cell should be optimally matched, and the load impedance should be fully modulated.

These experimental results clearly demonstrate the superior performance of the proposed amplifier. The proposed amplifier is the most suitable one for an application requiring high linearity and efficiency.

REFERENCES

- [1] S. C. Cripps, *RF Power Amplifiers for Wireless Communications*. Norwood, MA: Artech House, 1999.
- [2] J. Cha, Y. Yang, B. Shin, and B. Kim, "An adaptive bias controlled power amplifier with a load-modulated combining scheme for high efficiency and linearity," in *IEEE MTT-S Int. Microwave Symp. Dig.*, vol. 1, Jun. 2003, pp. 81–84.
- [3] Y. Yang, J. Cha, B. Shin, and B. Kim, "A microwave Doherty amplifier employing envelope tracking technique for high efficiency and linearity," *IEEE Microw. Compon. Lett.*, vol. 13, no. 9, pp. 370–372, Sep. 2003.
- [4] F. H. Raab, "Efficiency of Doherty RF power-amplifier systems," *IEEE Trans. Broadcast.*, vol. BC-33, no. 3, pp. 77–83, Sep. 1987.
- [5] W. H. Doherty, "A new high efficiency power amplifier for modulated waves," *Proc. IRE*, vol. 24, no. 9, pp. 1163–1182, Sep. 1936.
- [6] Y. Yang, J. Cha, B. Shin, and B. Kim, "A fully matched N -way Doherty amplifier with optimized linearity," *IEEE Trans. Microw. Theory Tech.*, vol. 51, no. 3, pp. 986–993, Mar. 2003.
- [7] B. Kim, Y. Yang, J. Yi, J. Nam, Y. Y. Woo, and J. Cha, "Efficiency enhancement of linear power amplifier using load modulation technique," in *Int. Microwave and Optical Technology Symp. Dig.*, Jun. 2001, pp. 505–508.
- [8] D. M. Upton, "A new circuit topology to realize high efficiency, high linearity and high power microwave amplifiers," in *Proc. RAWCON'98*, Aug. 1998, pp. 317–320.
- [9] S. C. Cripps, *Advanced Techniques in RF Power Amplifier Design*. Norwood, MA: Artech House, 2002.
- [10] Y. Zhao, M. Iwamoto, L. E. Larson, and P. M. Asbeck, "Doherty amplifier with DSP control to improve performance in CDMA operation," in *IEEE MTT-S Int. Microwave Symp. Dig.*, vol. 2, Jun. 2003, pp. 687–690.
- [11] J. Cha, J. Kim, B. Kim, J. S. Lee, and S. H. Kim, "Highly efficient power amplifier for CDMA base stations using Doherty configuration," in *IEEE MTT-S Int. Microwave Symp. Dig.*, Jun. 2004, pp. 553–556.
- [12] S. M. Wood, R. S. Pengelly, and M. Suto, "A high power high efficiency UMTS amplifier using a novel Doherty configuration," in *Proc. RAWCON'03*, Aug. 10–13, 2003, pp. 329–332.
- [13] Y. Yang, J. Yi, Y. Y. Woo, and B. Kim, "Optimum design for linearity and efficiency of microwave Doherty amplifier using a new load matching technique," *Microwave J.*, vol. 44, no. 12, pp. 20–36, Dec. 2001.
- [14] B. Shin, J. Cha, J. Kim, Y. Y. Woo, J. Yi, and B. Kim, "Linear power amplifier based on 3-way Doherty amplifier with predistorter," in *IEEE MTT-S Int. Microwave Symp. Dig.*, Jun. 2004, pp. 2027–2030.
- [15] M. Iwamoto, A. Williams, P. Chen, A. G. Metzger, L. E. Larson, and P. M. Asbeck, "An extended Doherty amplifier with high efficiency over a wide power range," *IEEE Trans. Microw. Theory Tech.*, vol. 49, no. 12, pp. 2472–2479, Dec. 2001.
- [16] N. Srirattana, A. Raghavan, D. Heo, P. E. Allen, and J. Laskar, "Analysis and design of a high efficiency multistage Doherty power amplifier for WCDMA," in *Eur. Microwave Conf. Dig.*, vol. 3, Oct. 2003, pp. 1337–1340.



Jangheon Kim was born in Jeonju, Korea, in 1980. He received the B.S. degree in electronics and information engineering from Chon-buk National University, Chonju, Korea, in 2003, and is currently working toward the Ph.D. degree at the Pohang University of Science and Technology (POSTECH), Pohang, Gyungbuk, Korea.

His current research interests include highly linear and efficient RF power-amplifier design and linearization techniques.



Jeonghyeon Cha was born in Gimje, Korea, in 1975. He received the B.S. degree in electronics and information engineering from Chon-buk National University, Chonju, Korea, in 2001, and is currently working toward the Ph.D. degree at the Pohang University of Science and Technology (POSTECH), Pohang, Gyungbuk, Korea.

His current research interests include RF power amplifier design, linearization techniques, and efficiency-improving techniques.



Ildu Kim was born in Kwangju, Korea, in 1981. He received the B.S. degree in electronics and information engineering from Chon-nam National University, Kwangju, Korea, in 2004, and is currently working toward the Ph.D. degree at the Pohang University of Science and Technology (POSTECH), Pohang, Gyungbuk, Korea.

His current research interests include RF power-amplifier design and linearity and efficiency improvement techniques.



Bumman Kim (S'77–M'78–SM'97) received the Ph.D. degree in electrical engineering from Carnegie–Mellon University, Pittsburgh, PA, in 1979.

From 1978 to 1981, he was engaged in fiber-optic network component research with GTE Laboratories Inc. In 1981, he joined the Central Research Laboratories, Texas Instruments Incorporated, where he was involved in development of GaAs power field-effect transistors (FETs) and monolithic microwave integrated circuits (MMICs). He has developed a

large-signal model of a power FET, dual-gate FETs for gain control, high-power distributed amplifiers, and various millimeter-wave MMICs. In 1989, he joined the Pohang University of Science and Technology (POSTECH), Pohang, Gyungbuk, Korea, where he is a Namko Professor with the Department of Electrical Engineering, and Director of the Microwave Application Research Center, where he is involved in device and circuit technology for RF integrated circuits (RFICs). He was a Visiting Professor of electrical engineering with the California Institute of Technology, Pasadena, in 2001. He has authored over 200 technical papers.

Dr. Kim is a member of the Korean Academy of Science and Technology and the Academy of Engineering of Korea. He is an associate editor for the *IEEE TRANSACTIONS ON MICROWAVE THEORY AND TECHNIQUES* and a Distinguished Lecturer of the IEEE Microwave Theory and Techniques Society (IEEE MTT-S).